

Comparison of Belgian and Dutch results from backward-in-time ATMs for the fictitious nuclear detonation case of NPE 2024

Michiel de Bode¹, Pieter De Meutter², Astrid Kloosterman¹, Andy Delcloo³, Sander Tijm⁴

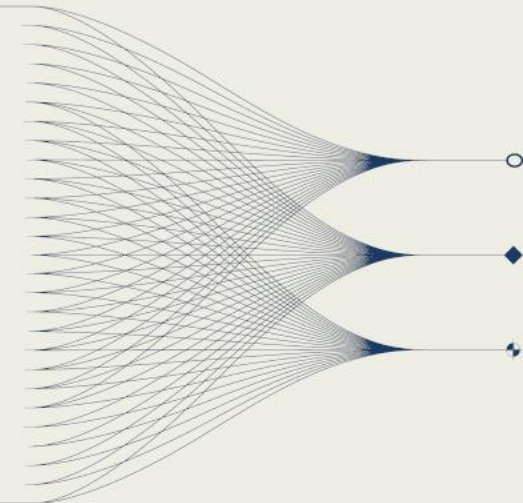
- 1 National Institute for Public Health and the Environment
- 2 Belgian nuclear research centre
- 3 Royal Meteorological Institute of Belgium
- 4 Royal Netherlands Meteorological Institute



INTRODUCTION AND MAIN RESULTS

In the framework of the National Data Centre Preparedness Exercise 2024, the Dutch and Belgian National Data Centres present and compare their methods for linking radionuclide observations with a (fictitious) event of interest. It involves the use of SHERLOC (Dutch) on one hand, and IFS+FLEXPART and FREAR (Belgian) on the other hand.

Both models show good overlap in their dispersion and location of the source. Nonetheless, there are major differences in the correlation results and the spread over the selected extent.





Introduction and case description

With regard to CTBT-relevant events, the Netherlands, Belgium and Luxemburg often work together, as three relatively small countries. Within this collaboration it is important to properly understand each other's models and its capacities, therefore, the effort was made by the RIVM and SCK CEN to both run the NPE 2024 detection case.

The case consists of waveform (seismic and infrasound) measurements and measurements of Xenon isotopes in Europe as displayed in **Figure 1 & 2**. With these observations the participating parties had to determine whether a Treaty violation occurred.

The waveform signals likely came from a location close to the Azores in the Atlantic ocean as depicted in **Figure 3**.

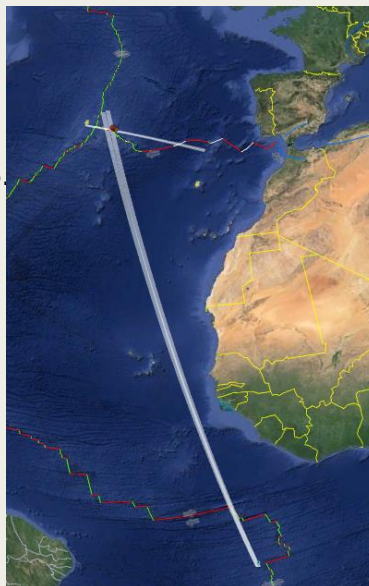


Figure 3: Estimated source location

Observations – NPE 2024

| # | Station | Nr | Start | | | | | Stop | | | | | Lon | Lat |
|------------|---------|---------|-------|----|----|-------|---------|------|----|-------|--|-------|-------|-----|
| # # # | | YYYY MM | DD | hh | mm | | YYYY MM | DD | hh | mm | | [deg] | [deg] | |
| "DEX33_27" | " | 001 | 2024 | 01 | 26 | 06 00 | 2024 | 01 | 27 | 06 0 | | 7.91 | 47.92 | |
| "DEX33_28" | " | 002 | 2024 | 01 | 27 | 06 00 | 2024 | 01 | 28 | 06 00 | | 7.91 | 47.92 | |
| "DEX33_29" | " | 003 | 2024 | 01 | 28 | 06 00 | 2024 | 01 | 29 | 06 00 | | 7.91 | 47.92 | |
| "DEX33_02" | " | 004 | 2024 | 02 | 01 | 06 00 | 2024 | 02 | 02 | 06 00 | | 7.91 | 47.92 | |
| "SEX_2904" | " | 005 | 2024 | 01 | 28 | 22 00 | 2024 | 01 | 29 | 04 00 | | 17.94 | 59.41 | |
| "SEX_2910" | " | 006 | 2024 | 01 | 29 | 04 00 | 2024 | 01 | 29 | 10 00 | | 17.94 | 59.41 | |
| "SEX_2916" | " | 007 | 2024 | 01 | 29 | 10 00 | 2024 | 01 | 29 | 16 00 | | 17.94 | 59.41 | |
| "SEX_2922" | " | 008 | 2024 | 01 | 29 | 16 00 | 2024 | 01 | 29 | 22 00 | | 17.94 | 59.41 | |
| "SEX_3004" | " | 009 | 2024 | 01 | 29 | 22 00 | 2024 | 01 | 30 | 04 00 | | 17.94 | 59.41 | |
| "SEX_3010" | " | 010 | 2024 | 01 | 30 | 04 00 | 2024 | 01 | 30 | 10 00 | | 17.94 | 59.41 | |
| "SEX_3016" | " | 011 | 2024 | 01 | 30 | 10 00 | 2024 | 01 | 30 | 16 00 | | 17.94 | 59.41 | |
| "SEX_3022" | " | 012 | 2024 | 01 | 30 | 16 00 | 2024 | 01 | 30 | 22 00 | | 17.94 | 59.41 | |
| "SEX_3104" | " | 013 | 2024 | 01 | 30 | 22 00 | 2024 | 01 | 31 | 04 00 | | 17.94 | 59.41 | |
| "SEX_3110" | " | 014 | 2024 | 01 | 31 | 04 00 | 2024 | 01 | 31 | 10 00 | | 17.94 | 59.41 | |
| "SEX_3116" | " | 015 | 2024 | 01 | 31 | 10 00 | 2024 | 01 | 31 | 16 00 | | 17.94 | 59.41 | |
| "SEX_3122" | " | 016 | 2024 | 01 | 31 | 16 00 | 2024 | 01 | 31 | 22 00 | | 17.94 | 59.41 | |

Figure 1: Measurements of Xe isotopes

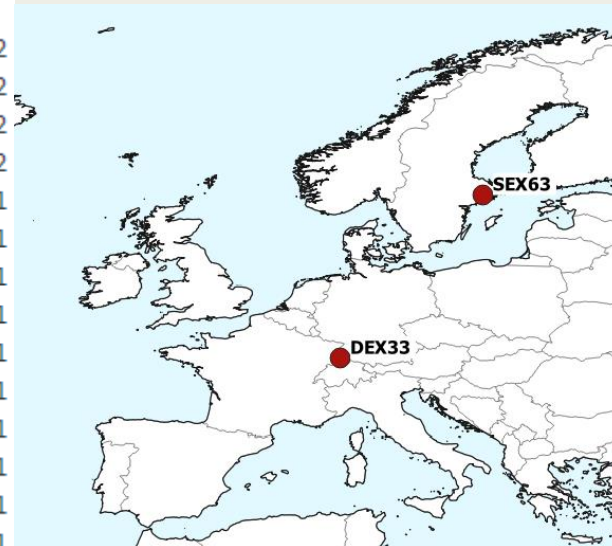


Figure 2: Measurement stations

Figure 1 has the observation intervals that are used by both the models. The information comes from two locations, the Swedish 'SEX63' observations with a six-hour sampling period and the German 'DEX33' observations with a daily sampling period.

The extent that will be shown here lies between 80°W – 10°E and 15°N – 70°N and are both calculated with data originating from the ECMWF.

Results of RIVM

The gaussian puff model NPK-PUFF is the default model used by the RIVM for the modelling of dispersion of harmful material with a focus on nuclear material and has since its introduction in 1998 (Uijt de Haag et al., 1998) it has been improved and expanded. With the extension of SHERLOC (Tomas et al., 2021) it can also do backwards calculations. The modelling follows the puffs and uses a Gaussian distribution for both the horizontal and vertical concentration. It uses a Pearson correlation for the calculation for the agreement. The meteorological data originates from the ECMWF7 model with a 0.25° spatial resolution and a 3-hour temporal resolution. Using NPK-puff with the 16 observations leads to the backward calculation fields as seen in figure:

Figure 4 show the agreement within the domain until 20 January. It shows high values over the Atlantic ocean. With further zoom (not shown) three hot spots are distinguishable where one matches **Figure 3**'s origin. **Figure 5** show the moment when the maximum agreement was calculated in hours before the start of the simulation. **Figure 6** shows all the individual releases of SHERLOCs calculation. Where PSR means "Possible Source Region".

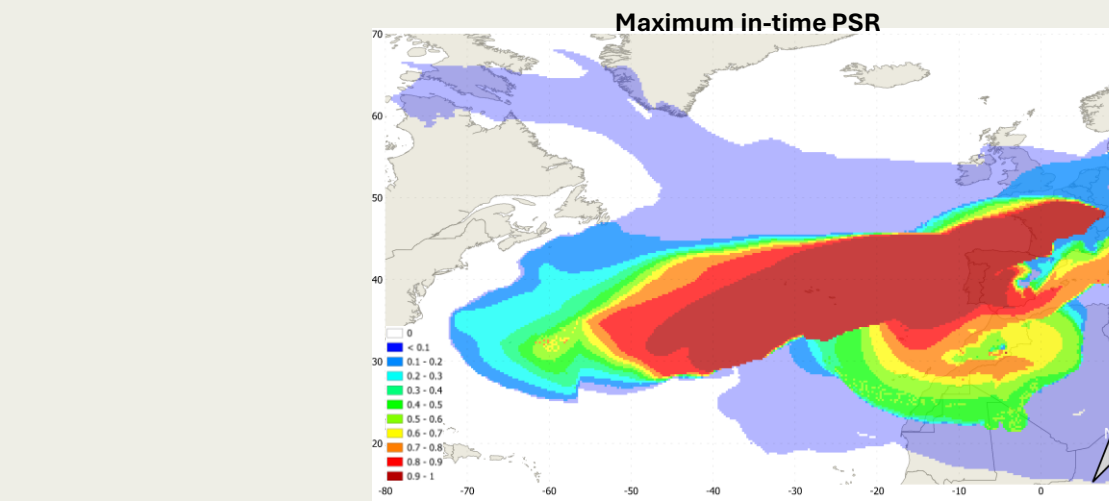


Figure 4: Maximum correlation back to 20-jan-2024

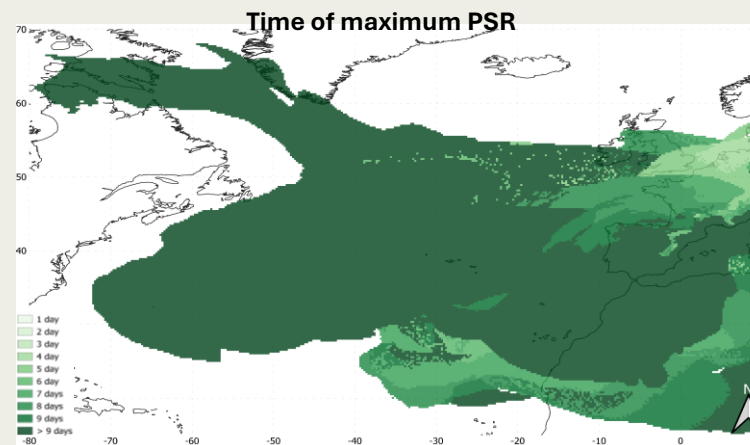


Figure 5: Time of maximum correlation, in days until the start of simulation

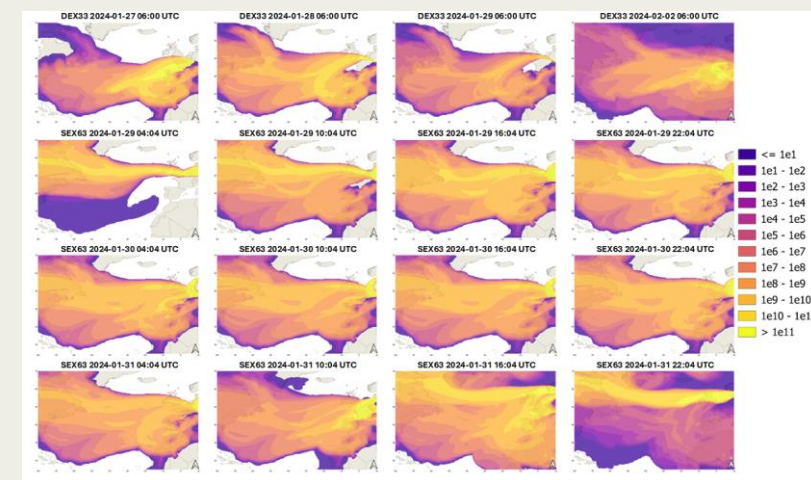


Figure 6: Simulation of individual measurements, see fig1

Presentation of results SCK CEN

The Lagrangian particle dispersion model Flexpart (Stohl et al. 2005, Pissot et al., 2019) is used by the Belgian NDC to simulate activity concentrations in forward mode and source-receptor sensitivities in backward mode. Here, for each of the 16 selected observations, a backward simulation was conducted (Seibert and Frank, 2004). Flexpart was coupled with three-hourly numerical weather prediction data from the Integrated Forecasting System of ECMWF extracted at 0.5° horizontal grid spacings. The resulting 16 4D source-receptor sensitivity fields were then used to create the PSR (possible source region) product, which is obtained by taking the correlation between the observed Xe-133 activity concentration and the source-receptor sensitivity for each spatio-temporal grid box. In a next step, for each grid box, the maximum-in-time is taken.

The results are shown in **Figure 7** for the Pearson correlation and **Figure 8** for the Spearman Rank correlation. The timestep of maximum Pearson correlation is given in **Figure 9**, with lower numbers denoting further backward in time. The Field-Of-Regard for each backward simulation is shown in **Figure 10**.

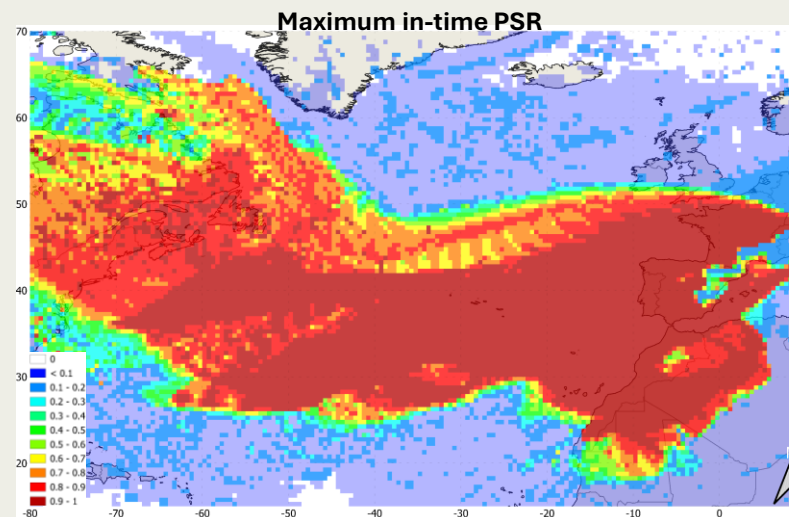


Figure 7: Maximum in-time PSR, Pearson correlation

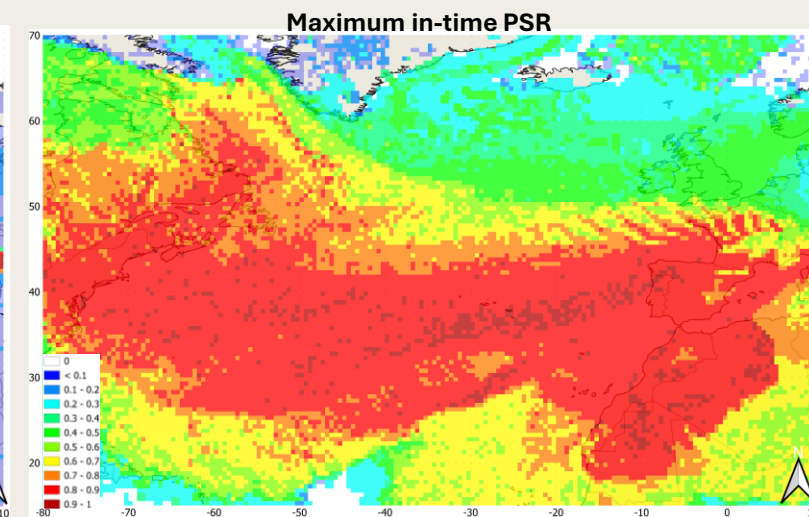


Figure 8: Maximum in-time PSR, Spearman correlation

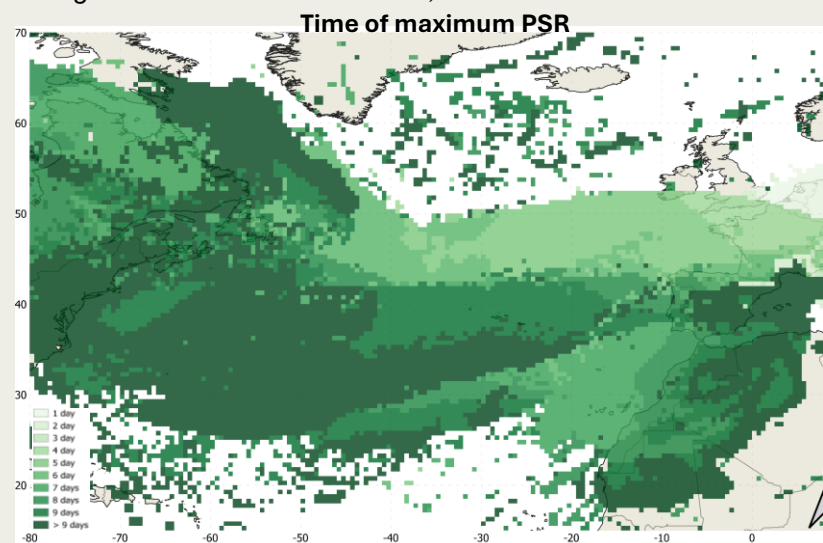


Figure 9: Time of maximum correlation, in days until the start of simulation

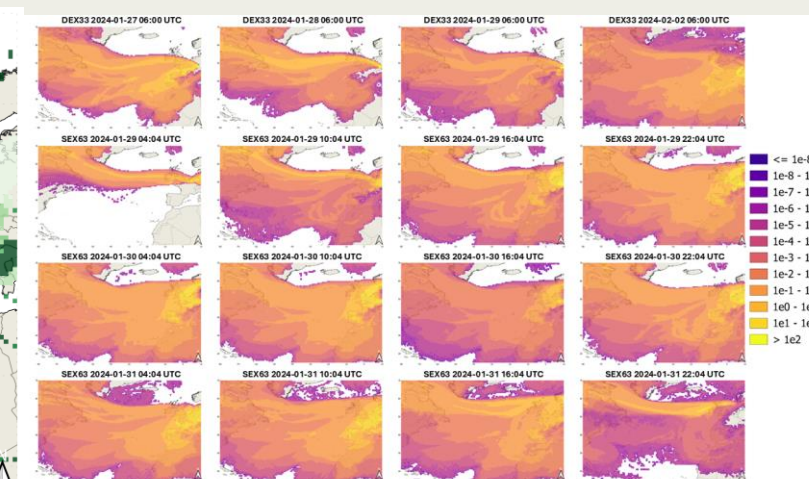


Figure 10: Simulation of individual measurements, see fig.

Comparison of results

Table 1: Comparison of RIVM and two SCK CEN correlations

| Min correlation | Spearman overlap [%] | Pearson overlap [%] |
|-----------------|----------------------|---------------------|
| 0.5 | 30.13 | 45.44 |
| 0.75 | 32.61 | 36.09 |
| 0.9 | 9.88 | 37.95 |
| 0.95 | 0.00 | 23.89 |

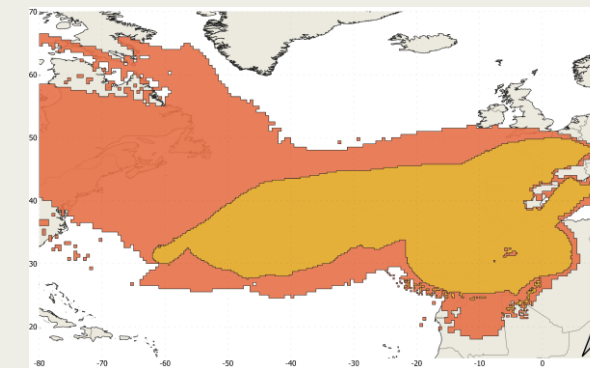


Figure 11: Example of Figure of Merit in Space

Using the figure of merit space (FMS) an attempt was made to quantify the agreement of PSR between the two models and their methods. **Figure 11** shows an example of the FMS calculation. Where the small area indicates the location found by both models and the large area only found by a single model. **Table 1** shows how much overlap the models have, where overlap is the fraction of small area over the large area.

Besides, we also did a direct comparison of backward-in-time model output. The general pattern of transport and dispersion seems to be comparable. **Figure 12** shows the calculations as done for two observations as illustration. They are calculated slightly different, therefore, have a slightly different legend, but can be interpreted the same.

The results of RIVM features sharper gradients, which seems to be an effect of the dispersion of puffs with a Gaussian distribution instead of dispersing particles that are directly influenced by the turbulence.

Figure 13 show a comparison of two time series and the correlation by both models, where it is shown that the RIVM model does not always give correlations while the SCK CEN model does, when there are plumes coming over.

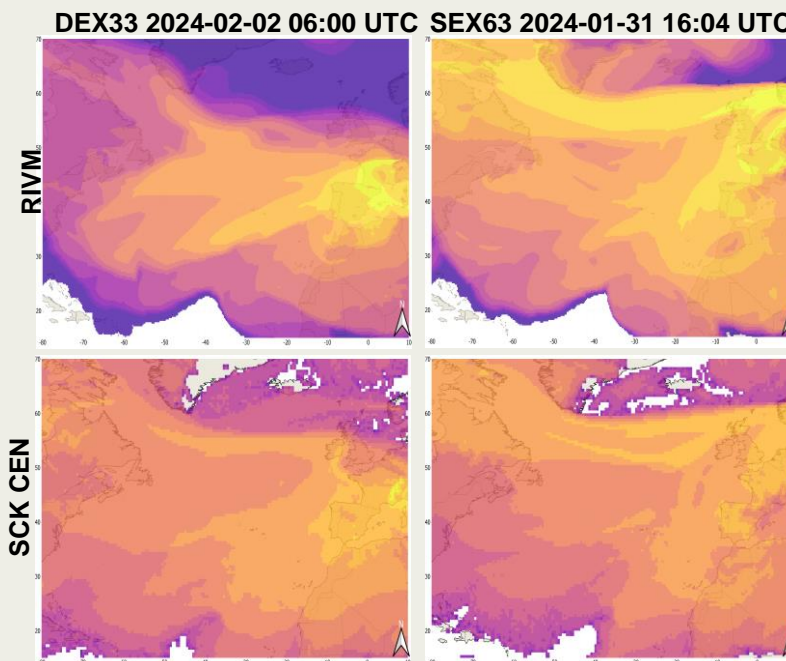


Figure 12: Comparison of two different retro-plumes

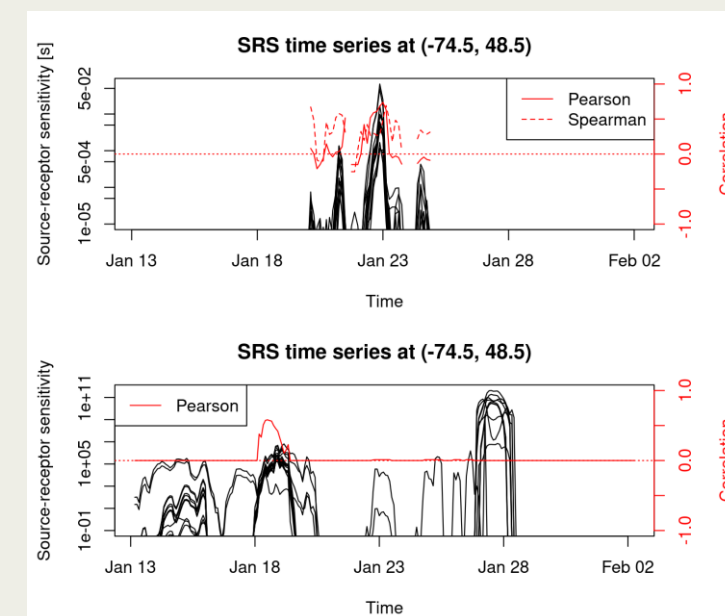


Figure 13: SRS and correlation over time at a point of interest, for both models.



Conclusions

Both models have comparable results but show differences that are inherent to the models, and both have researched slightly different things.

Results of the RIVM generally have more concentrated values, a few possibilities are currently researched by the RIVM and SCK CEN. A possibility is the type of model, as a Gaussian plume parameterization instead of transporting single particles might reduce the spreading of the values as only a core is moved. While the RIVM model applies a process to reduce the impact of this difference every 6 hours.

Other things that were noticed are that the Pearson has smaller areas with higher correlation than that the Spearman correlation does.

It leads to better understanding of our models and what they do, making future improvements and research easier.

Future steps

The Dutch and Belgian NDCs will continue collaboration on CTBT-relevant events by exchanging analyses and information, and by conducting joint research on an ad-hoc basis.

It is useful to continue the search for methods to accurately compare different models when they calculate the same thing in different ways. Therefore, new methods and techniques for comparison shall be explored. E.g., a manner to help with studying the difference in displacement of the particles is to focus on a few points and see if there are values for those moments, and how they change over time.

It has become clear that the RIVM model still has some teething problems left and were highlighted during this comparison. They will improve on these point before a new larger scale investigation is started.

References

Pisso, I., Sollum, E., Grythe, H., Kristiansen, N. I., Cassiani, M., Eckhardt, S., ... & Stohl, A. (2019). The Lagrangian particle dispersion model FLEXPART version 10.4. *Geoscientific Model Development*, 12(12), 4955-4997.

Seibert, P., & Frank, A. (2004). Source-receptor matrix calculation with a Lagrangian particle dispersion model in backward mode. *Atmospheric Chemistry and Physics*, 4(1), 51-63.

Stohl, A., Forster, C., Frank, A., Seibert, P., & Wotawa, G. (2005). The Lagrangian particle dispersion model FLEXPART version 6.2. *Atmospheric Chemistry and Physics*, 5(9), 2461-2474.

Tomas, J. M., Peereboom, V., Kloosterman, A., & van Dijk, A. (2021). Detection of radioactivity of unknown origin: Protective actions based on inverse modelling. *Journal of Environmental Radioactivity*, 235-236, 106643. <https://doi.org/10.1016/j.jenvrad.2021.106643>

Uijt de Haag, P. A. M., Geertsema, G. T., Kroonenberg, F., & Aldenkamp, F. J. (1998). *Invoering van het luchtverspreidingsmodel NPK-PUFF, versie 1.0, voor toepassing in de NPK-organisatie* (Publication No. 610057008; p. 32). RIVM. <https://www.rivm.nl/publicaties/invoering-van-luchtverspreidingsmodel-npk-puff-versie-10-voor-toepassing-in-npk>